AD-A068 193 GEORGIA INST OF TECH ATLANTA ELECTROMAGNETIC EFFECTI--ETC F/G 20/14
NEAR-FIELD THEORY AND TECHNIQUES FOR WIDEBAND RADIATING SYSTEMS--ETC(U)
APR 79 B J COWN, C E RYAN DAAG29-78-C-0029
UNCLASSIFIED GIT/EED-A-2179-ITR-1 ARO-15646.1-EL NL

| OF |
ADA
068193

END
DATE
FILMED
6-79
DDC

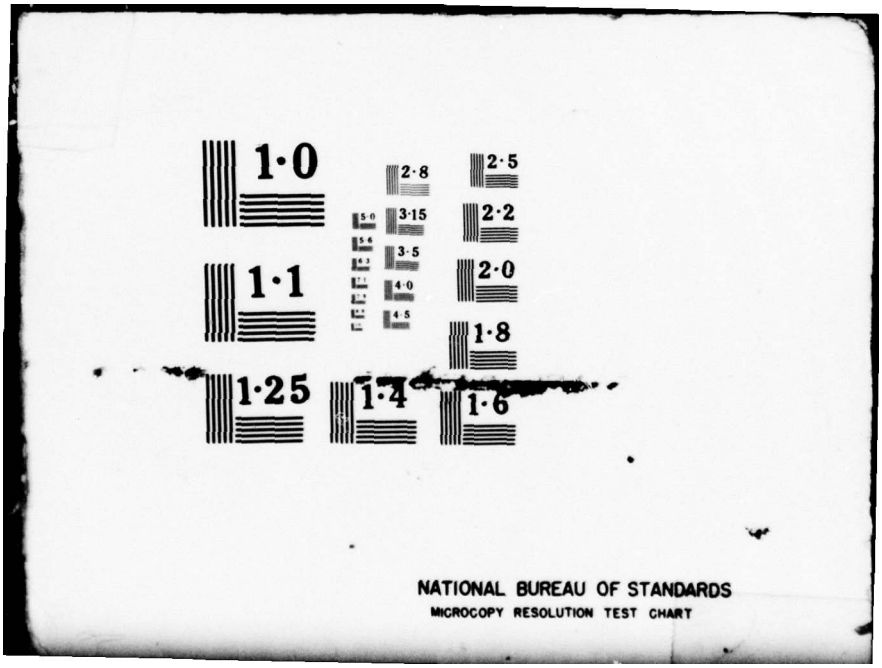
1·0
1·1
1·25
1·4
1·6
1·8
2·0
2·2
2·5
2·8
3·15
3·5
4·0
4·5
NATIONAL BUREAU OF STANDARDS
MICROCOPY RESOLUTION TEST CHART

LEVEL II

12

INTERIM TECHNICAL REPORT NO. 1

PROJECT A-2179

NEAR-FIELD THEORY AND TECHNIQUES FOR WIDEBAND RADIATING SYSTEMS AT IN-BAND AND OUT-OF-BAND FREQUENCIES

By

B. J. Cown and C. E. Ryan, Jr.

CONTRACT NO. DAAG29-78-C-0029

JULY 1978 through JANUARY 1979

Prepared for

U. S. ARMY RESEARCH OFFICE
P. O. BOX 12211
RESEARCH TRIANGLE PARK
NORTH, CAROLINA 27709

GEORGIA INSTITUTE OF TECHNOLOGY
Engineering Experiment Station
Atlanta, Georgia 30332

GTEES

1979

Unclassified

SECURITY CLASSIFICATION OF PAGE (When Data Entered) (18) ARO

REPORT DOCUMENTATION PAGE

READ INSTRUCTIONS BEFORE COMPLETING FORM

1. REPORT NUMBER (19) 15646.1-EL	2. GOVT ACCESSION NO.
3. RECIPIENT'S CATALOG NUMBER	
4. TITLE (and Subtitle) (6) Near-Field Theory and Techniques for Wideband Radiating Systems at In-Band and Out-of-Band Frequencies	5. TYPE OF REPORT & PERIOD COVERED: Technical
	6. PERFORMING ORG. REPORT NUMBER
7. AUTHOR(s) (10) B. J. Cown, C. E. Ryan, Jr. (12) 45p.	8. CONTRACT OR GRANT NUMBER(s) (15) DAAG29-78-C-0029
9. PERFORMING ORGANIZATION NAME AND ADDRESS: Georgia Institute of Technology, Engineering Experiment Station, Atlanta, Georgia 30332	10. PROGRAM ELEMENT, PROJECT, TASK AREA & WORK UNIT NUMBERS
11. CONTROLLING OFFICE NAME AND ADDRESS: U. S. Army Research Office, P. O. Box 12211, Research Triangle Park, NC 27709	(11) 12. REPORT DATE: Apr 79 13. NUMBER OF PAGES: 38
14. MONITORING AGENCY NAME & ADDRESS(if different from Controlling Office) (14) GIT/EED-A-2179-ITR-1	15. SECURITY CLASS. (of this report): Unclassified 15a. DECLASSIFICATION/DOWNGRADING SCHEDULE

16. DISTRIBUTION STATEMENT (of this Report)

Approved for public release; distribution unlimited.

(9) Interim technical rept. no 1, 15 Jun 78-31 Jan 79

17. DISTRIBUTION STATEMENT (of the abstract entered in Block 20, if different from Report)

18. SUPPLEMENTARY NOTES

The view, opinions, and/or findings contained in this report are those of the author(s) and should not be construed as an official Department of the Army position, policy, or decision, unless so designated by other documentation.

19. KEY WORDS (Continue on reverse side if necessary and identify by block number)

Electromagnetic radiation	in-band frequencies
Near-filed theory	out-of- band frequencies
Antennas	radiation patterns
Wide Band Radiating Systems	radiating systems

411 115

20. ABSTRACT (Continue on reverse side if necessary and identify by block number)

This report summarizes the results achieved to date in the research program concerning wideband in-band and out-of-band radiating systems. The research program is primarily devoted to a basic study of methods to characterize wideband radiating systems performance and the applications of near-field techniques to such characterizations. Accordingly, the overall research program is divided into four major tasks that are designed to provide a systematic approach to understanding and solving the complex electromagnetic effectiveness problems inherent in out-of-band phenomena.

DD FORM 1 JAN 73 1473 EDITION OF 1 NOV 65 IS OBSOLETE

Unclassified

SECURITY CLASSIFICATION OF THIS PAGE (When Data Entered)

INTERIM TECHNICAL REPORT NO. 1

PROJECT A-2179

NEAR-FIELD THEORY AND TECHNIQUES FOR WIDEBAND RADIATING SYSTEMS AT IN-BAND AND OUT-OF-BAND FREQUENCIES

By

B. J. Cown and C. E. Ryan, Jr.

Contract No. DAAG29-78-C-0029

July 1978 through January 1979

Prepared for

U.S. Army Research Office
P.O. Box 12211
Research Triangle Park, North Carolina 27709

Prepared by

Electromagnetic Effectiveness Division
Systems and Techniques Laboratory
Engineering Experiment Station
Georgia Institute of Technology
Atlanta, Georgia 30332

FOREWORD

The research on this program was performed by personnel of the Electromagnetic Effectiveness Division of the Systems and Techniques Laboratory of the Engineering Experiment Station at the Georgia Institute of Technology, Atlanta, Georgia 30332. Dr. C. E. Ryan, Jr. served as the Project Director. This program is sponsored by the Army Research Office, P.O. Box 12211, Research Triangle Park, North Carolina 27709, and is designated by Georgia Tech as Project A-2179. This Interim Technical Report covers the period from 15 June 1978 through 31 January 1979.

Respectfully submitted,

C. E. Ryan Jr.

C. E. Ryan, Jr.
Project Director

Approved:

Fred L. Cain

Fred L. Cain
Chief,
EM Effectiveness Division

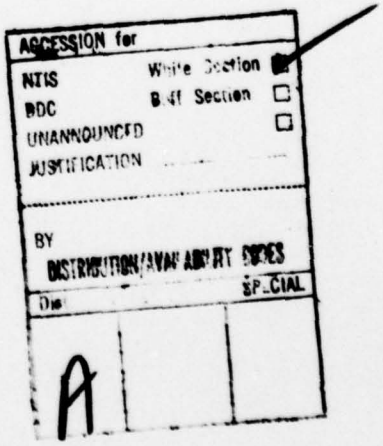

TABLE OF CONTENTS

LIST OF FIGURES

LIST OF FIGURES
(continued)

SECTION I

INTRODUCTION

The material contained herein summarizes the progress and results achieved to date in the research program concerning wideband in-band and out-of-band radiating systems. The research program is primarily devoted to a basic study of methods to characterize wideband radiating systems performance and the applications of near-field techniques to such characterizations. Accordingly, the overall research program is divided into four major tasks that are designed to provide a systematic approach to understanding and solving the complex electromagnetic effectiveness problems inherent in out-of-band phenomena. The four major tasks are defined as follows.

Task 1. Provide a near-field methodology to characterize electromagnetic emitter radiation patterns at in-band and out-of-band frequencies for wide bandwidth radiators. The objective of this task is to develop the appropriate theory and equations based on statistical analysis techniques for efficient characterization of wideband radiators.

Task 2. Theoretically relate the radiation pattern characterization methodology to the data needs of electromagnetic spectrum usage optimization analysis. The objective of this task is to relate the near-field derived wideband antenna characterization to the performance of transmitting and receiving systems which co-exist in the same EM environment.

Task 3. Provide the methodology to assess the effects of system devices (i.e., higher-order mode generation) on the radiation pattern. The objective of this task is to determine a method whereby the pattern effects of higher-order modes which are generated by system devices at out-of-band frequencies can be assessed.

Task 4. Investigate the impact of site effects on the near-field antenna analysis technology. The objective of this task is to extend

the existing monochromatic spectrum scattering matrix analysis to study antenna siting effects on the wideband and out-of-band performance of radiating systems.

The research efforts on the various tasks are to be conducted in accordance with the program schedule presented on Page 3. Accordingly, the efforts thus far have been directed toward Task 1.

The approach taken to accomplish the objectives of Task 1 consists of research efforts on the following three subtasks.

(a) Develop the theory for both in-band and out-of-band frequencies for deriving statistical average far-field patterns from wideband or pulsed near-field measurements. This study will concentrate on methods to derive valid far-zone pattern statistics by either defining a minimum set of required near-field data or by developing optimum near-field data processing techniques such as averaging or time domain pulse synthesis.

(b) Based upon the theoretical studies, methods of efficiently characterizing both wideband continuous-wave and pulsed radiators using near-field measurement techniques will be devised and studied. The basic limitations of these methods will be identified, and the expected accuracy of each of the techniques will be assessed.

(c) Based upon the theoretical studies, a numerical simulation which will be applicable to various antenna types, such as reflector and phased-array antennas, will be developed to demonstrate that valid statistical far-field pattern distributions can be obtained from near-field measurements.

Preliminary theoretical results of the research efforts conducted thus far are presented and discussed in Section II. The results of a statistical numerical simulation of linear phased array performance are presented in Section III. These numerical results are used to validate the analytically derived statistical patterns and to show the general trends of the out-of-band antenna performance which must be taken into consideration in the analysis. Finally, Section IV presents a summary of the work performed to date and scheduled future efforts.

PROGRAM SCHEDULE

Out-of-Band EMC Measurement Techniques

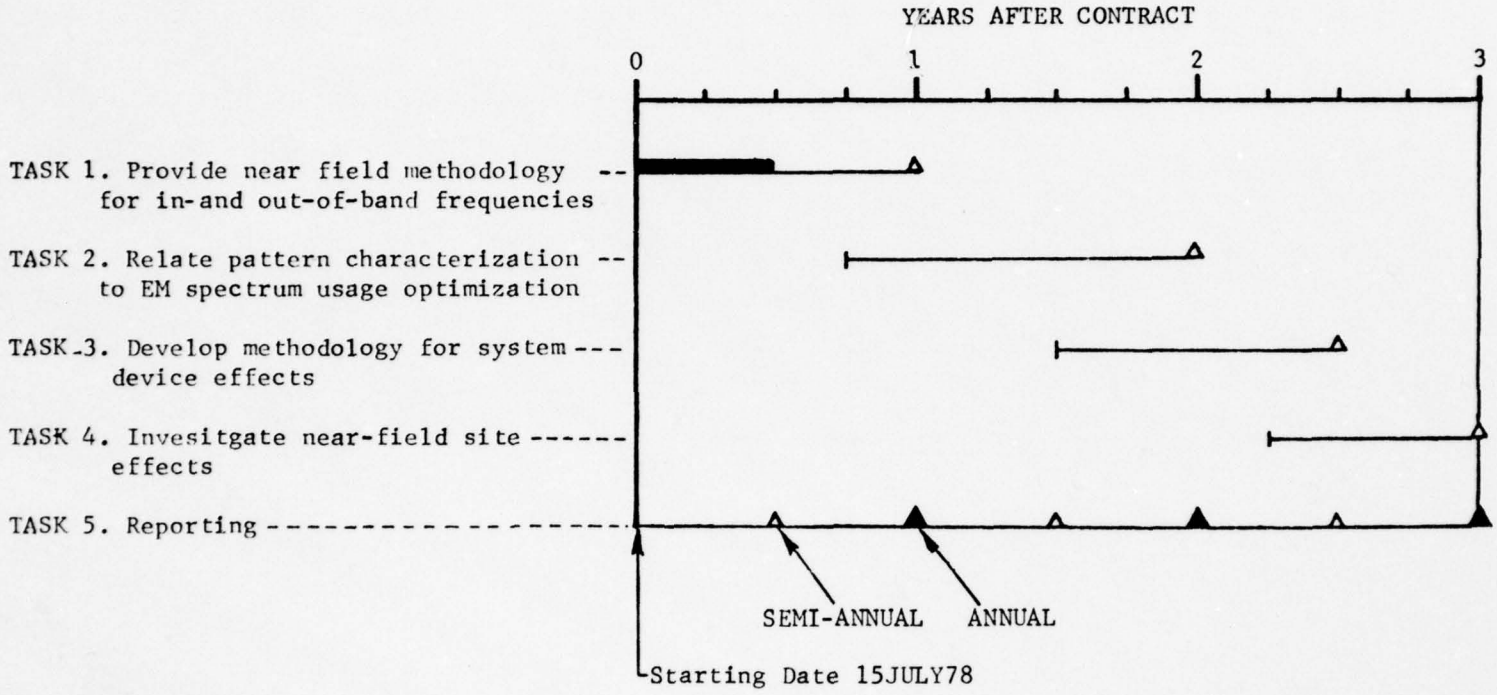

SECTION II

THEORETICAL DEVELOPMENT OF STATISTICAL EQUATIONS

A. Introduction

The electromagnetic radiation characteristics of a pulsed or wideband radiating system can be predicted and described by conventional electromagnetic analysis techniques if all of the system variables behave in a deterministic manner. However, there is a strong possibility that some of the system variables for pulsed or wideband radiating systems may behave in a random manner if the feed network can support multi-mode energy propagation at any of the relevant frequencies in the operational frequency band. It is known from both theory and experiment that the radiated fields will also exhibit random behavior [1-4]. Consequently, statistical analysis techniques must be applied to predict and describe the radiation characteristics. Statistical analyses involve the application of certain mathematical operations, notably certain kinds of integrations or summations, to the initially deterministic conventional equations. Consequently, the resulting statistical equations for the antenna radiation patterns involve all of the deterministic variables of a system plus the statistical parameters of the variables that are random.

The primary thrust of the theoretical efforts thus far has been to develop the equations relating the far-field out-of-band antenna pattern characteristics to the electromagnetic field quantities obtained from near-field antenna measurements. These initial preliminary analyses have been conducted for a one-dimensional radiator in order to gain insight into the nature and complexity of the statistical aspects of the problem. However, extension of the techniques to the two-dimensional case is straightforward, albeit tedious.

B. Frequency Domain Statistics

The analysis has been conducted for the linear array of waveguide elements depicted in Figure 1. The array is assumed to be either pulsed or operated over a finite frequency band. The frequency spectrum is

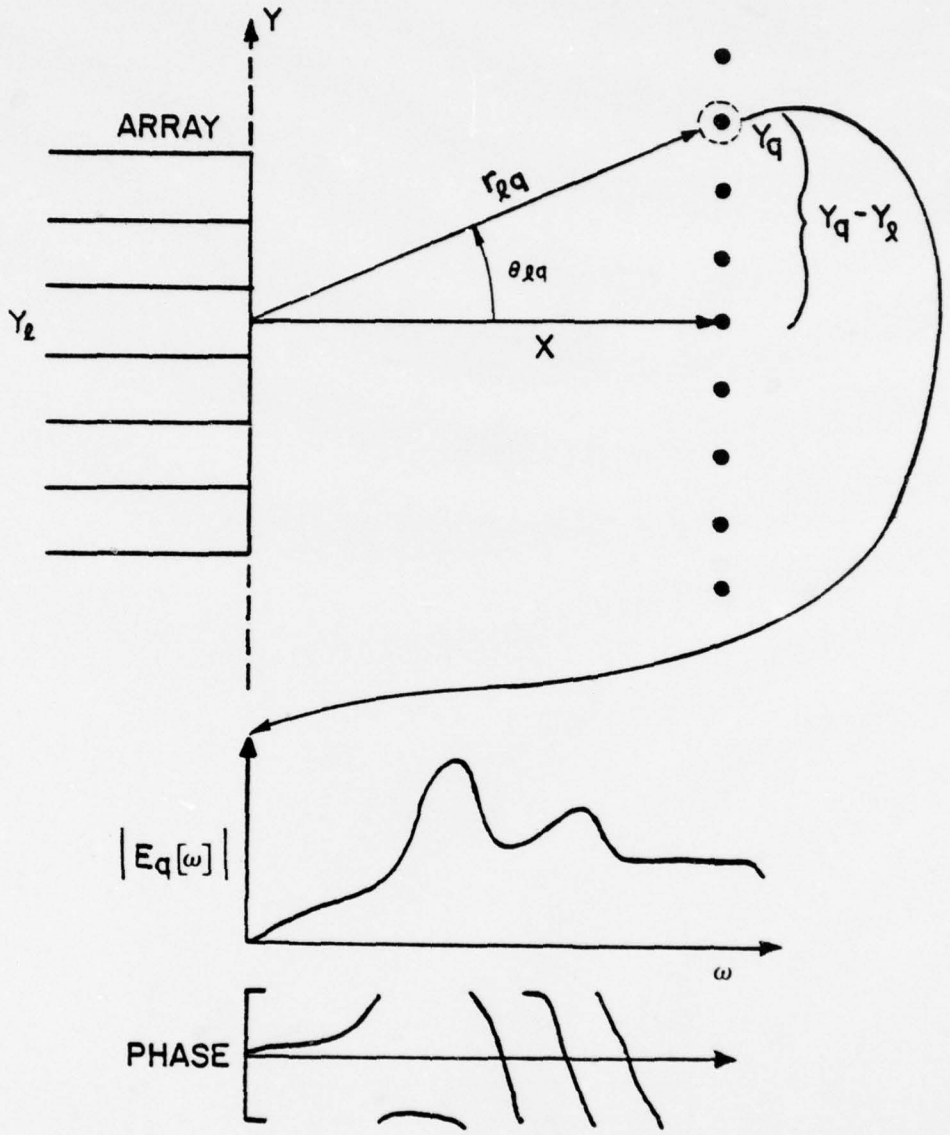

Figure 1. Sketch depicting a linear array of waveguide elements and hypothetical out-of-band amplitude and phase responses at a near-field measurement point.

assumed to contain some components which can be propagated in higher-order mode field configurations in the waveguide elements. A convenient starting point in the analysis is to first write down the appropriate equations for a non-random antenna measurement situation. The analysis of randomly-excited antennas can then subsequently be conducted based on the initially deterministic equations and statistical analysis techniques.

The electric field produced on the near-field measurement plane located at $x = x_o$ is the superposition of the radiation fields of the individual element radiators. It is assumed that the measurement plane is located at a distance x_o that is greater than or equal to the far-field distance of each element radiator. The electric field produced at a near-field measurement point due to the multi-moding array of waveguide elements may be written as

$$E_q(\omega) = \sum_{\ell} \sum_{m} a_{\ell}^{m}(\omega) h_{\ell}^{m}(\omega, \phi_{\ell q}) \frac{\exp\left[-j \frac{\omega}{c} r_{\ell q}\right]}{r_{\ell q}}, \qquad (1)$$

where $\omega = 2\pi \times$ frequency,

A_{ℓ}^{m} = complex mode coefficient for the m^{th} mode in the ℓ^{th} element,

h_{ℓ}^{m} = far-field electric field pattern of the m^{th} mode of the ℓ^{th} element,

$\phi_{\ell q}$ = angular location of the q^{th} measurement point with respect to the center of the ℓ^{th} element,

c = speed of light in vacuo, and

$r_{\ell q}$ = magnitude of the radius vector from the center of the ℓ^{th} element to the q^{th} measurement point.

The plots of amplitude and phase shown near the bottom of Figure 1 depict either (1) the electric field versus frequency as the array input signal is swept over a specified frequency band or (2) the complex frequency spectrum of a radiated pulse. In either case, different

results would be obtained at different measurement points. The frequency spectrum of the time pulse is obtained via the Fourier transform of the pulse, which is

$$E_q(\omega) = \sum_n E_q(t_n) \exp\left[-j\omega t_n\right] \quad , \tag{2}$$

where $E_q(t_n)$ is the time-domain response.

The far-field electric field is obtained as the discrete Fourier transform of the near-field electric field. Thus, the far-field electric field is given as

$$E(\omega,\phi) = \sum_q E_q(\omega) \exp\left[-j \frac{\omega}{c} \sin(\phi) Y_q\right] \quad , \tag{3}$$

where Y_q = y-coordinate of the q^{th} measurement point,

ϕ = azimuth angle of the far-field observation point, and

where E_q is a previously defined by Equation (1). A factor (1/r), where r is the distance from the center of the measurement plane to the far-field observation point, has been suppressed in Equation (3) and subsequent equations.

The power density in the far-field of the antenna is obtained by multiplying Equation (3) by its complex conjugate. The resulting equation for the power density $P(\omega,\phi)$ is thence

$$P(\omega,\phi) \equiv E^*(\omega,\phi)E(\omega,\phi) =$$

$$\sum_{q'} \sum_q E^*_{q'}(\omega) E_q(\omega) \exp\left[j \frac{\omega}{c} \sin(\phi) \left(Y_{q'} - Y_q\right)\right] \quad . \tag{4}$$

Equations (1) through (4) are the well-known basic equations for analyzing deterministic (non-random) antenna patterns utilizing the frequency domain approach. The temporal (time) behavior of the electric field is obtained via the Fourier transform with respect to frequency. The corresponding analysis of a randomly-excited array

antena primarily involves the application of certain mathematical operations to these same equations, as described in the following paragraphs.

The plots shown in Figure 1 can be interpreted as representing the measured response obtained from one experiment involving a randomly-excited antenna. Successive experiments would yield different responses. Consequently, a randomly excited antenna has many possible near-field distributions, spectral responses, and far-field patterns. The amount of near-field data required to characterize a randomly-excited antenna will be much greater than the amount of data required to characterize a comparable deterministic antenna unless suitable statistical analysis can be devised to reduce the data requirements.

The statistical average value of the far-field power density is written as

$$\langle P(\omega,\phi)\rangle = \sum_{q'}\sum_{q}\langle E^{*}_{q'}(\omega,\phi)\ E_{q}(\omega,\phi)\rangle\ \exp\left[j\ \frac{\omega}{c}\ \sin(\phi)(Y_{q'}-Y_{q})\right], \tag{5}$$

where the angular brackets denote the statistical average value [5]. The angular brackets are shorthand notation for integrals of the type

$$\langle W(\chi)\rangle = \int_{\xi_1}\cdots\int_{\xi_n} W(\chi|\xi_1\cdots\xi_n)\,f(\xi_1\cdots\xi_n)\,d\xi_1\cdots d\xi_n\ , \tag{6}$$

where χ = a non-random variable,

ξ = random variables, and

$f(\xi)$ = probability density function for the random variables.

Similarly, the statistical average value of the (complex)electric field is

$$\langle E(\omega,\phi)\rangle = \sum_{q}\langle E_{q}(\omega)\rangle\ \exp\left[-j\ \frac{\omega}{c}\ \sin\ (\phi)Y_{q}\right]\ . \tag{7}$$

The electric field is, of course, a complex valued function and is therefore not an observable quantity. However, the statistical average

value and higher-order statistical moments are well defined quantities [5]. In particular, the statistical average value of the complex electric field E_q is defined as

$$\langle E_q(\omega) \rangle = \langle U_q(\omega) \rangle - j \langle V_q(\omega) \rangle \quad . \tag{8}$$

where U_q and V_q denote the real and imaginary parts, respectively, of E_q. U_q and V_q are defined in the conventional manner as

$$U_q(\omega) = A_q(\omega) \cos\left[\alpha_q(\omega)\right] \quad , \text{ and} \tag{9}$$

$$V_q(\omega) = A_q(\omega) \sin\left[\alpha_q(\omega)\right] \quad . \tag{10}$$

where $A_q(\omega)$ = relative amplitude (real number) of the electric field at q, and

$\alpha_q(\omega)$ = relative phase of the electric field at q.

Thus, a knowledge of the average values of the real and imaginary parts of the near-field electric field over the measurement plane permits the computation of the average far-field electric field as the Fourier transform of the average near-field electric field.

The average power density is related to the product $< E^* > < E >$, where the symbol * denotes complex conjugation, as

$$\langle P(\omega,\phi) \rangle = \langle E^*(\omega,\phi) \rangle \langle E(\omega,\phi) \rangle + C_{E^*,E}(\omega,\phi) \quad . \tag{11}$$

The symbol $C_{E^*,E}$ denotes the covariance function and is defined as

$$C_{E^*,E}(\omega,\phi) = \langle E^*(\omega,\phi) E(\omega,\phi) \rangle - \langle E^*(\omega,\phi) \rangle \langle E(\omega,\phi) \rangle \quad . \tag{12}$$

The equation for the far-field covariance function can be derived for the linear array via straightforward algebraic manipulations. The

resulting equation is

$$C_{E^*,E}(\omega,\phi) = \sum_q \gamma^2_q(\omega,\phi) + \sum_{q'} \sum_q \gamma_{q'}(\omega)\gamma_q(\omega)R_{q',q}(\omega)\exp\left[j\frac{\omega}{c}\sin(\omega)(Y_{q'}-Y_q)\right], \tag{13}$$

where γ_q denotes the standard deviation of the near-field electric field at q and $R_{q',q}$ denotes the cross-correlation coefficient for the electric field at q and the conjugate of the electric field at q'.

The standard deviation γ_q is a real number and is equal to the square root of the sum of the variances of the real and imaginary parts of E_q. Accordingly, γ_q is written as

$$\gamma_q(\omega) = \sqrt{[\sigma_u(\omega)]^2_q + [\sigma_v(\omega)]^2_q}\ , \tag{14}$$

where $[\sigma_u(\omega)]_q$ = standard deviation of the real part of E_q, and

$[\sigma_v(\omega)]_q$ = standard deviation of the imaginary part of E_q.

The cross-correlation coefficients $R_{q',q}$ are defined as the complex numbers obtained via the equation

$$R_{q',q}(\omega) = \frac{C_{q',q}(\omega)}{\gamma_{q'}(\omega)\ \gamma_q(\omega)}\ , \tag{15}$$

where the numerator of Equation (15) is referred to as the cross-covariance function. The cross-covariance of the electric field at q is

$$\begin{aligned} C_{q',q}(\omega) = &\left\{\left[\langle U_{q'}(\omega)U_q(\omega)\rangle - \langle U_{q'}(\omega)\rangle\langle U_q(\omega)\rangle\right]\right. \\ &\left.+\left[\langle V_{q'}(\omega)V_q(\omega)\rangle - \langle V_{q'}(\omega)\rangle\langle V_q(\omega)\rangle\right]\right\} \\ &+j\left\{\left[\langle V_{q'}(\omega)U_q(\omega)\rangle - \langle V_{q'}(\omega)\rangle\langle U_q(\omega)\rangle\right]\right. \\ &\left.-\left[\langle U_{q'}(\omega)V_q(\omega)\rangle - \langle U_{q'}(\omega)\rangle\langle V_q(\omega)\rangle\right]\right\}\ . \end{aligned} \tag{16}$$

The rigorous analysis of the far-field statistical average power pattern for a given frequency is seen from Equation (7) through (16) to require computation of the following near-field statistical quantities:

(1) statistical average value of the real and imaginary parts of the near-field electric field at all measurement points,

(2) the standard deviation of the real and imaginary parts of the near-field electric field at all measurement points, and

(3) the cross-correlation coefficients of the near-field electric field at all different measurement points.

In a near-field measurement situation, these quantities could be determined by computing the "sample" average values and standard deviations obtained from repeated trials. The sample average value [5] of a random variable W is defined as

$$\langle W \rangle = \frac{1}{N} \sum_{n} W_n \quad , \tag{17}$$

where W_n is the value of W obtained in the n^{th} trial, and N is the number of trials. Similarly, the sample standard deviation σ_w is defined as

$$\sigma_W = \sqrt{\frac{1}{N} \sum_{n} [W_n - \langle W \rangle]^2} \quad . \tag{18}$$

The measurement procedure for a CW antenna might proceed as follows. With the probe positioned at the measurement point q, sweep the frequency of the transmitting test antenna over the frequency band, recording the relative received power level in dB and the relative phase angle in degrees, on magnetic tape or disc at preselected frequencies in the band. Repeat this procedure, say, 10 times. Reposition the probe to the next sample point and repeat the measurement process until all desired measurements are completed.

Computation of the required near-field statistical parameters for each discrete frequency is then carried out via computer programs. The far-field statistical average power pattern given by Equation (11) is computed with the aid of a computer program employing the Fast Fourier Transform algorithm. However, the computations are likely to become

prohibitively time consuming and expensive and may exceed active computer core requirements if it is necessary to compute all of the correlation coefficients. It is very likely that the correlation coefficients decrease rapidly as a function of distance between different sample points. Consequently, it may be possible to greatly reduce the number of correlation coefficient computations. It is anticipated that measurement experience with near-field out-of-band radiating system will provide engineering guidelines for selecting the size of the correlation region that is needed for accurate pattern calculations. Estimates of the size of the correlation region can also be derived in terms of assumed correlation coefficients of the random mode excitation coefficients within the radiating system proper.

It should be noted that statistical correlation between the modes in different elements of an array antenna will be a function of mutual coupling between the array elements. The degree of the correlation between the signals in different elements is proportional to the degree of mutual coupling between the elements. Consequently, the magnitude of the correlation coefficients and the size of correlation region may vary considerably with in-band operating conditions such as in-band design scan angle. However, in the absence of mutual coupling, each element is functionally independent of all other elements, and there is therefore no mechanism for correlation between inter-element mode coefficients. That is, the random variations in the mode excitation coefficients in different elements are statistically independent and therefore are statistically uncorrelated in the limit of zero mutual coupling.

If the intra-element mode excitation coefficients are also statistically independent, the cross-correlation coefficients of the entire near-field electric field will all be zero and the statistical average power pattern is then computed as

$$\langle P(\omega,\phi)\rangle = \langle E^*(\omega,\phi)\rangle \langle E(\omega,\phi)\rangle + \sum_q \gamma_q^2(\omega) \quad , \qquad (19)$$

where all symbols are as previously defined. Moreover, the probability density function for this important special case has been previously derived. A knowledge of the probability density function permits computation of the standard deviation and any other higher order statistical moments of the far-field power pattern. The equation for the probability density function is derived in Reference 3 and is presented below as

$$f[P(\omega,\phi)] = \frac{1}{\tau(\omega,\phi)} \exp\left[-\frac{P(\omega,\phi) + \eta^2(\omega,\phi)}{\tau(\omega)}\right] \cdot I_o[\beta(\omega,\phi)] \quad , \tag{20}$$

where $f[P(\omega,\phi)]$ = probability density function for the far-field power density,

$$\eta^2(\omega,\phi) = \left\langle E^*(\omega,\phi)\right\rangle \left\langle E(\omega,\phi)\right\rangle \quad , \tag{21}$$

$$\tau(\omega) = \sum_{q'} \gamma^2_{q}(\omega) \quad , \tag{22}$$

$I_o[\cdot]$ = Modified Bessel function of the first kind and order zero, and (23)

$$\beta(\omega,\phi) = \frac{\eta(\omega,\phi)\sqrt{P(\omega,\phi)}}{\frac{1}{2}\tau(\omega)} \quad .$$

Preliminary analyses indicate that the probability density function for the near-field power density has the same form as Equation (20). However, the parameters η, τ, and β are functions of the deterministic variables ω, x_o, Y_q, and ϕ_{pq} in the near-field case rather than (ω,ϕ) as in the far-field case. Of course, the parameters η, τ, and β are functions of the statistical parameters of the mode statistics for both the near-field and the far-field situations.

The average value and standard deviation of the far-field power density are readily obtained from Equation (20) by evaluating the integrals

$$\int_0^\infty P\, f[P]\, dP \quad , \quad \text{and} \tag{24}$$

$$\int_0^\infty [P - \langle P \rangle]^2 f[P]\, dP \quad , \tag{25}$$

respectively. The integrations can be performed with the aid of Laplace transform techniques and the resulting expressions for the average value $P(\omega,\phi)$ and standard deviation $\sigma_P(\omega,\phi)$ are, respectively,

$$\langle P(\omega,\phi) \rangle = \eta^2(\omega,\phi) + \tau(\omega) \quad , \tag{26}$$

$$\sigma_P(\omega,\phi) = \left[[\tau(\omega)]^2 + 2[\tau(\omega)]\eta^2(\omega,\phi) \right]^{1/2} \quad . \tag{27}$$

The statistical average complex frequency transfer function for the antenna system can also be obtained with the aid of the statistical Equation (6). A knowledge of the statistical average complex frequency transfer function allows computation of the statistical average time domain response of the antenna system. The average transfer function is computed as

$$\langle B(\omega,\phi) \rangle = \frac{\langle E(\omega,\phi) \rangle}{H(\omega)} \quad , \tag{28}$$

where $H(\omega)$ is either the complex frequency spectrum of the input time pulse to a pulsed system or simply the input test frequency spectrum for a CW system. The statistical average complex far-field electric field $E'(\omega,\phi)$ for a different input spectrum $H'(\omega')$ is just

$$\langle E'(\omega,\phi) \rangle = \langle B(\omega,\phi) \rangle H'(\omega) \quad . \tag{29}$$

The average time domain response $E'(t,\phi)$ is computed as the Fourier transform of Equation (29). Hence,

$$\langle E'(t,\phi)\rangle = \frac{1}{2\pi}\sum_{n}\langle B(\omega_n,\phi)\rangle H'(\omega_n)\exp[j\omega_n t] \quad . \tag{30}$$

C. Time Domain Statistics

The time-domain behavior of a pulsed antenna system can be obtained with the aid of the preceding frequency-domain equations and the Fourier transform with respect to frequency. In particular, the time dependent statistical average complex far-field electric field may be written as

$$\langle E(t,\phi)\rangle = \frac{1}{2\pi}\sum_{n}\langle E(\omega_n,\phi)\rangle\exp[j\omega_n t] \quad . \tag{31}$$

In analogy with the techniques described previously for computing average power density, the statistical average time dependent power density is written as

$$\langle P(t,\phi)\rangle = \langle E^*(t,\phi)\rangle\ \langle E(t,\phi)\rangle + \sum_{n}\xi_n^2 + \sum_{n'}\sum_{n}\xi_{n'}\ \xi_n\ R_{n'n}\exp\left[j(\omega_n-\omega_{n'})t\right] \quad , \tag{32}$$

where ξ_n = standard deviation of $E(\omega_n,\phi)$,

$\xi_{n'}$ = standard deviation of $E^*(\omega_{n'},\phi)$, and

$R_{n'n}$ = cross-correlation function of $E(\omega_n,\phi)$ and $E^*(\omega_{n'},\phi)$.

It should be noted that the cross-correlation function $R_{n'n}(\phi)$ appearing here is not a time correlation function but rather is a frequency-dependent correlation function for the electric fields at different frequencies.

A complete description of the statistics of the time dependent power density is possible if the probability density function can be

derived. In the limiting case where the mode excitation coefficients are statistically independent, preliminary analyses indicate that the probability density function for the time dependent power density for a pulse of moderate bandwidth has, approximately, the same analytical form as the probability density function for the frequency-dependent power density given previously in Equation (20). Further theoretical study is needed in order to derive the probability density function for pulse spectral beamwidths in the several gigahertz range.

D. Frequency-Averaged Statistical Average Antenna Patterns

The preceding discussions have addressed statistical averaging over randomly-varying variables. It may be meaningful to also average over frequency in some applications involving a CW radiating system of moderate bandwidth. The purpose of averaging over frequency is to obtain a single average pattern plus standard deviation that adequately describes the general radiation characteristics of the antenna. The single average pattern plus standard deviation replaces the large collection of patterns versus frequency that would otherwise be needed to characterize the antenna.

Two different methods for obtaining the frequency-averaged statistical pattern have been formulated. The most direct method for obtaining the frequency-averaged statistical average pattern is to first compute the statistical average pattern at selected frequencies and then arithmetically average the statistical average patterns. This process is described mathematically as

$$\langle\langle P(\omega,\phi)\rangle\rangle_{\omega} = \frac{1}{N}\sum_{n} P(\omega_n,\phi) \quad , \tag{33}$$

where N is the total number of selected frequencies and where frequency averaging is denoted by subscript ω on the outermost right-hand angular bracket. It is also possible to obtain the frequency-averaged statistical average pattern by first computing the deterministic frequency average and then computing the statistical average. This

process is described mathematically as

$$\left\langle \left\langle P(\omega,\phi) \right\rangle_{\omega} \right\rangle = \sum_{q'} \sum_{q} \left\langle D_{q',q} \right\rangle \exp\left[-j d_{q',q} \omega_c\right] \quad , \tag{34}$$

where

$$d_{q',q} = \frac{\sin(\phi)}{c} \left(Y_{q'} - Y_q\right) \quad , \text{ and} \tag{35}$$

$$\left\langle D_{q',q} \right\rangle = \frac{1}{2\pi N} \sum_{n} \left\langle E^*_{q'}(\omega_n,\phi) E_q(\omega_n) \right\rangle \exp\left[j d_{q',q} \omega_n\right] \quad . \tag{36}$$

The amount of computational labor required to compute frequency-average statistical average patterns is roughly equivalent for the two methods. It should be mentioned that the frequency averaging techniques discussed herein do not reduce the amount of near-field data that must be recorded. A reduction in the near-field data requirements can be accomplished at the expense of a nominal reduction in accuracy and detail in the far-field antenna pattern characterization. However, this tradeoff may well be justified in engineering applications. Numerical investigations have been initiated to study the suitability of using only the center-frequency statistical average pattern plus statistical standard deviation to characterize an out-of-band antenna over a 2-GHz bandwidth. Preliminary results are presented and discussed in the following section.

SECTION III
NUMERICAL SIMULATIONS

A. Introduction

Numerical simulations have been initiated with the aid of two existing computer programs AVPATT and RANPATT developed by Georgia Tech for analyzing linear random-out-of-band antenna systems. AVPATT computes statistical average patterns based on Equation (19). RANPATT computes individual random patterns based on Equation (5) and pseudo-random number generators. Both of these computer programs are coded in the ANSI FORTRAN IV computer language. The programs were originally written for execution on the old UNIVAC 1108 computing system. Necessary modifications have been completed making the programs compatible with the current CDC CYBER 74 computing system.

B. Out-of-Band Antenna Patterns

Statistical average antenna patterns and individual random antenna patterns have been computed for a randomly-excited linear array of waveguide elements. The in-band design frequency is 9.0 GHz and center-to-center element spacing is 0.53 λ_o where λ_o is the wavelength at 9.0 GHz. Both kinds of patterns were computed for out-of-band frequencies of 17 through 19 GHz in 0.5 GHz steps. Energy may be propagated in any combination of the five higher-order mode field configurations [6,7] that can exist in the WR-90 (X-band) waveguide at the aforementioned out-of-band frequencies. The transverse electric fields of the five possible propagating modes are depicted schematically in Figure 2. It is seen that the TE_{01} is polarized entirely transverse to the TE_{10} mode, and the TE_{11} and TM_{11} modes have components polarized transverse to the TE_{10} mode. The TE_{20} mode is polarized parallel with the TE_{10} mode. The out-of-band antenna patterns will have a cross-polarized component if energy is propagated in the TE_{01}, TE_{11}, and/or TM_{11} modes.

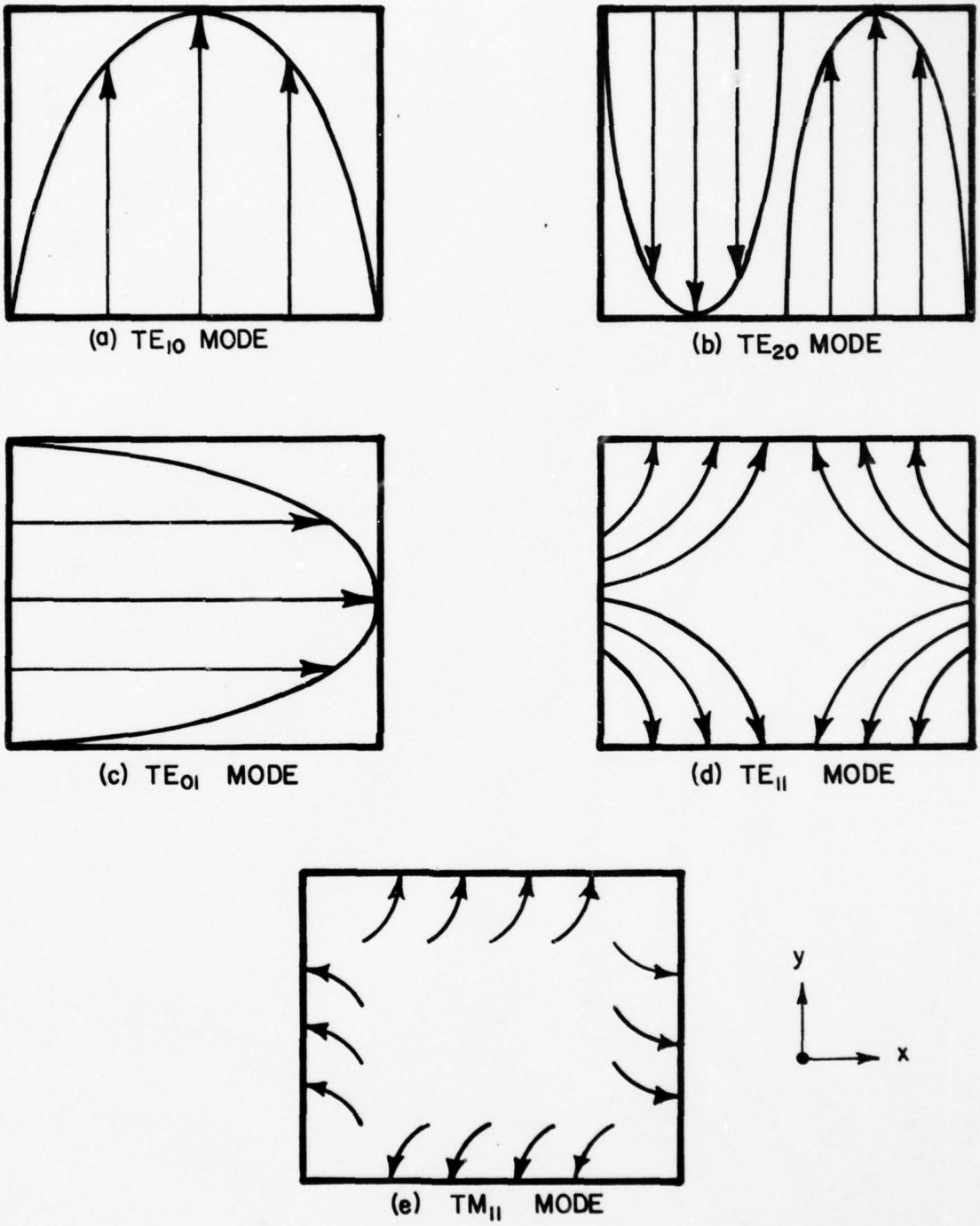

Figure 2. Sketch depicting the transverse electric fields of the five possible propagating out-of-band waveguide modes in WR-90 (x-band) waveguide at the operational frequency of 18 GHz.

The out-of-band antenna patterns shown in Figures 3 through 16 were computed for the out-of-band frequency of 18 GHz. Figures 3 through 10 involved energy propagation in all 5 modes. The statistical average value of the power flow in each mode is 0.2 watt. Note that the patterns shown in Figures 3 through 6 were computed for an in-band scan angle of zero degrees and the patterns shown in Figures 7 through 10 were computed for an in-band scan angle of -30 degrees. The statistical average patterns shown in Figures 11 and 12 involved energy propagation in only the TE_{10}, TE_{20}, and TE_{10} modes. The statistical average for the in-band scan angle of zero degrees power flow in each mode was 0.333 watt.

Comparisons of the statistical average patterns depicted in Figures 3, 5, 7, and 9 with their corresponding individual random patterns shown in Figures 4, 6, 8, and 10, respectively, indicate that the average patterns are a good descriptor of the general trends observed in the corresponding individual random antenna patterns. Comparison of the statistical average patterns depicted in Figures 11 and 12 with the statistical average patterns decpited in Figures 3 and 5 show that the overall shape of the patterns depends on the modal content. Referring to Figures 7 through 10, it is observed that the out-of-band mainbeam does not scan to the in-band scan angle of -30 degrees. All of the trends mentioned above are delineated and discussed in greater detail in References 3 and 4.

The out-of-band patterns shown in Figures 13 and 15 depict the superposition of the individual random antenna patterns at 17.0, 17.5, 18.0, 18.5, and 19.0 GHz for parallel and cross-polarization, respectively, followed by the same-sense statistical average pattern plus standard deviation for 18.0 GHz shown in Figures 14 and 16, respectively. The standard deviation line shown on Figures 14 and 16 for the sidelobe regions is an estimate based on the limiting value of Equation (27) in the sidelobe region and was manually graphed. The standard deviation equation will be incorporated in AVPATT in the near future.

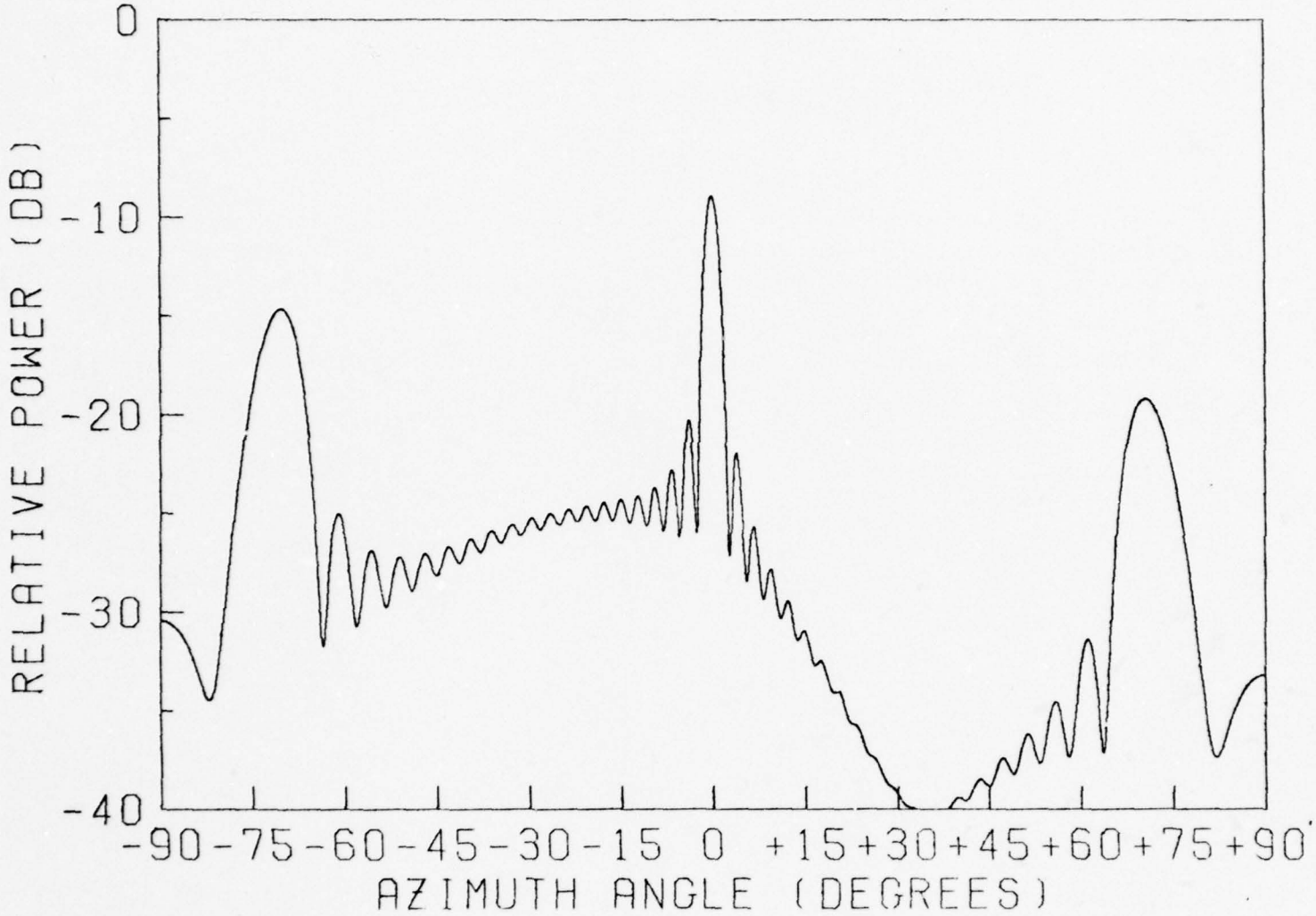

Figure 3. Statistical average out-of-band antenna pattern for parallel polarization for the in-band scan angle of zero degrees at 18.0 GHz involving the TE_{10}, TE_{20}, TE_{01}, TE_{11}, and TM_{11} waveguide modes.

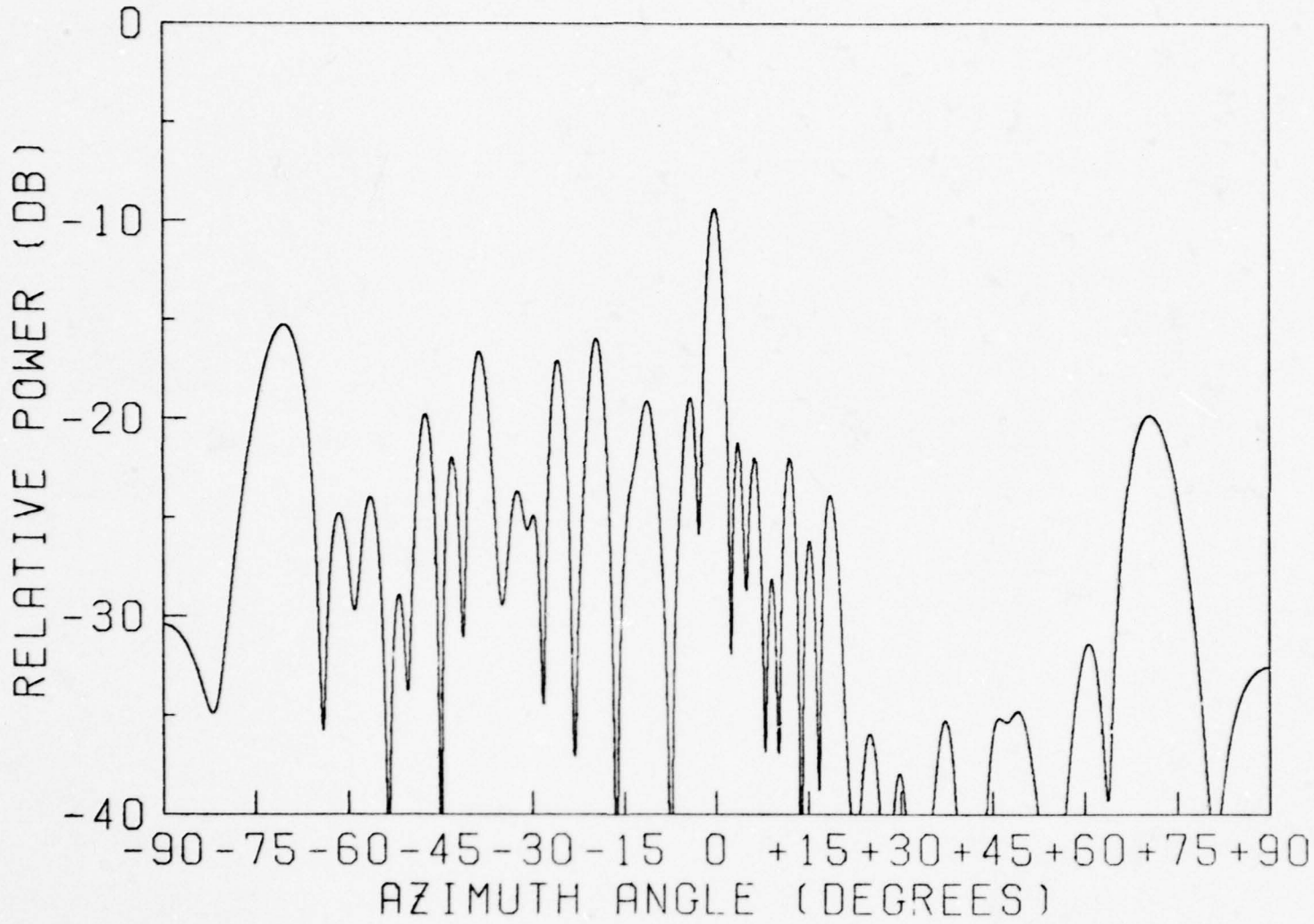

Figure 4. Individual random out-of-band antenna pattern for parallel polarization for the in-band scan angle of zero degrees at 18.0 GHz involving the TE_{10}, TE_{20}, TE_{01}, TE_{11} and TM_{11} waveguide modes.

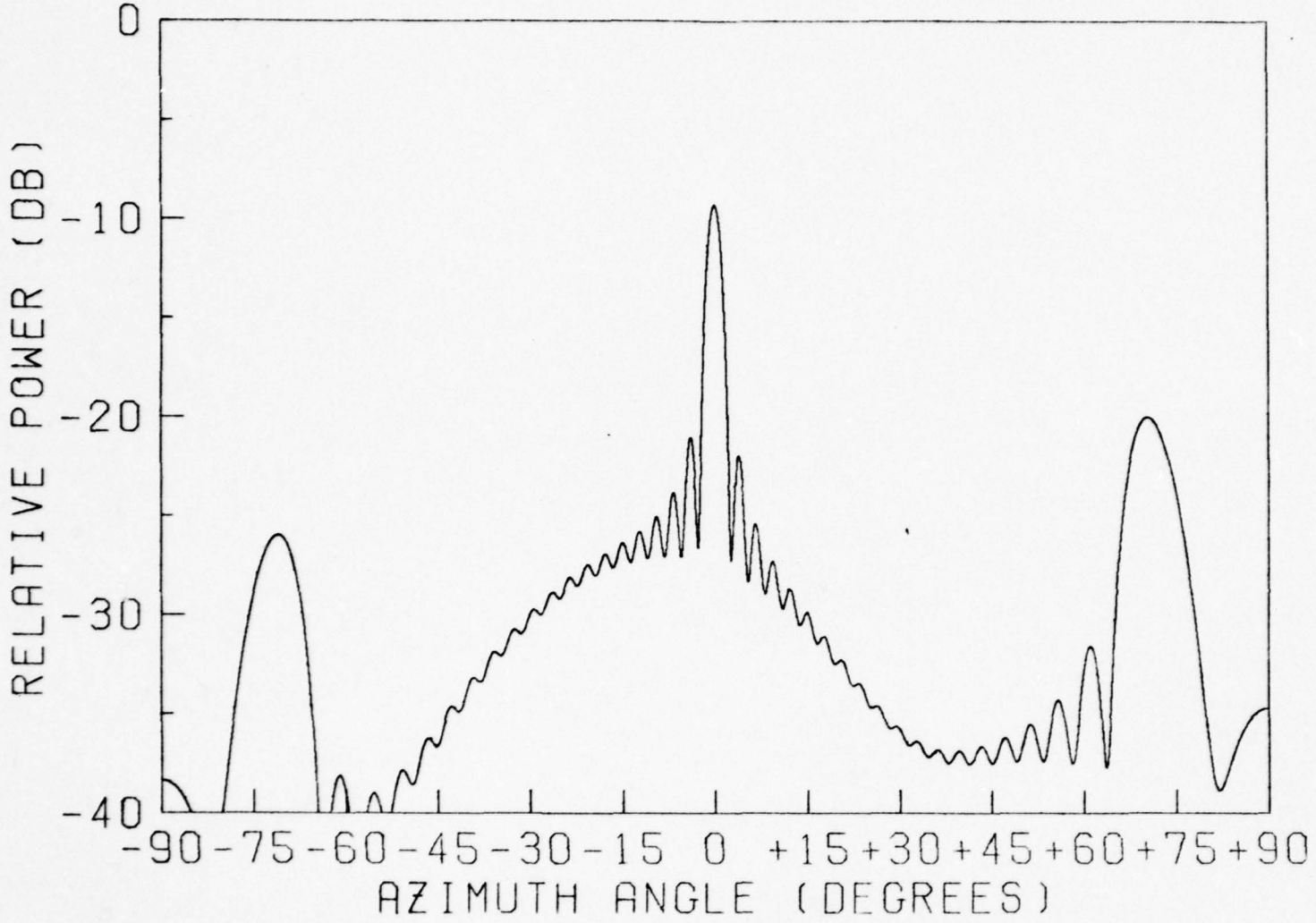

Figure 5. Statistical average out-of-band antenna pattern for cross polarization for the in-band scan angle of zero degrees at 18.0 GHz involving the TE_{10}, TE_{20}, TE_{01}, TE_{11}, and TM_{11} waveguide modes.

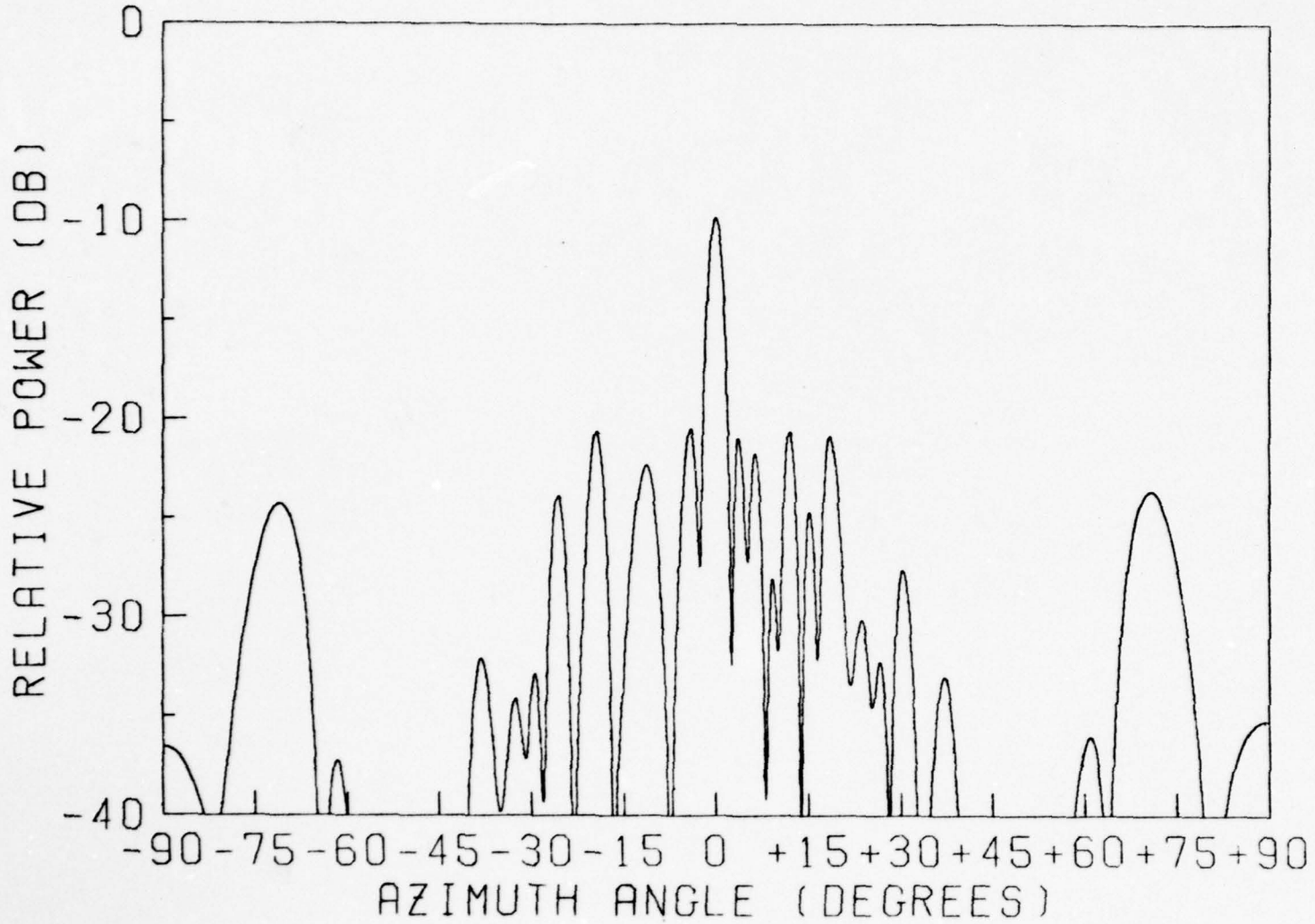

Figure 6. Individual random out-of-band antenna pattern for cross polarization for the in-band scan angle of zero degrees at 18.0 GHz involving the TE_{10}, TE_{20}, TE_{01}, TE_{11}, and TM_{11} waveguide modes.

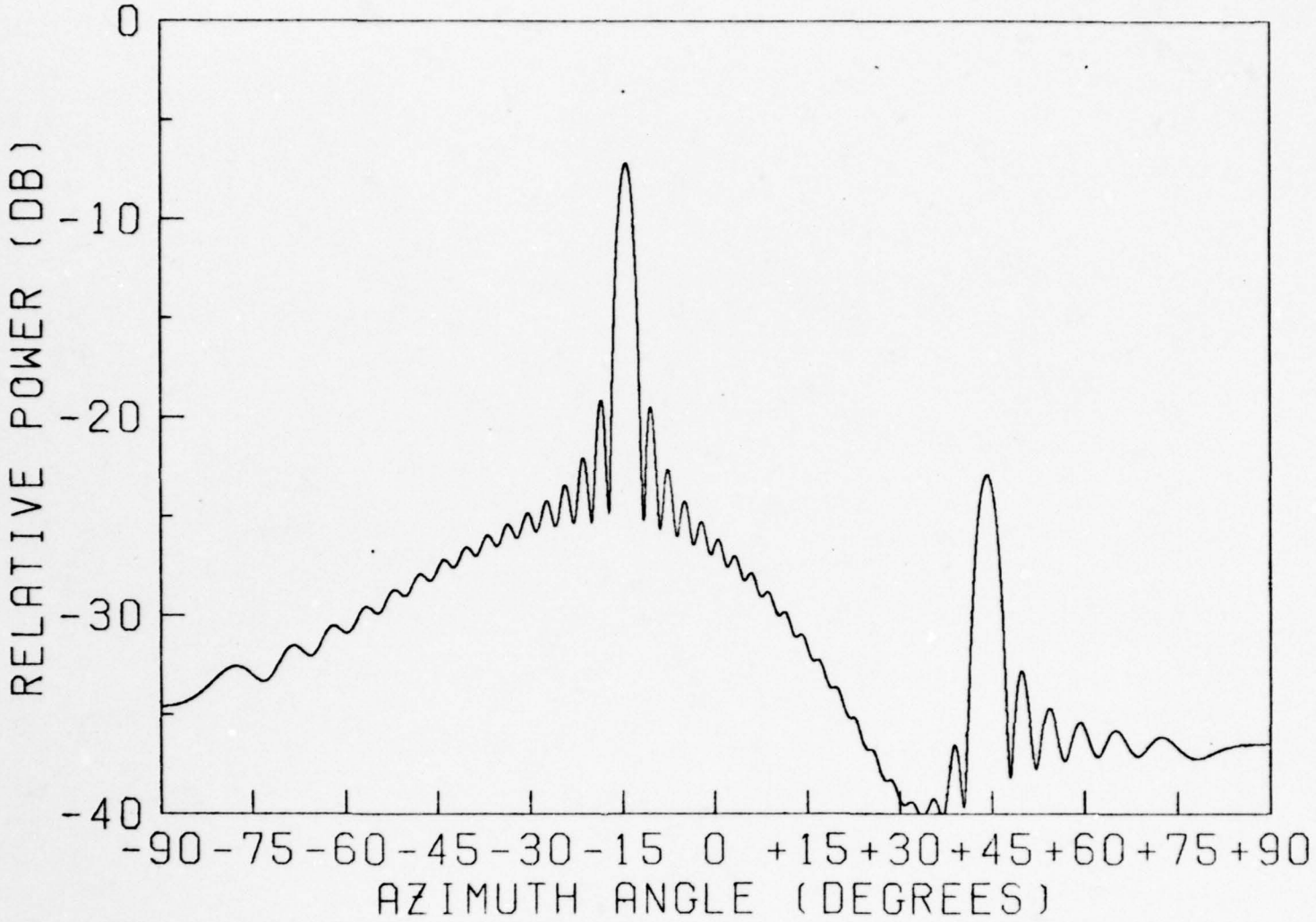

Figure 7. Statistical average out-of-band antenna pattern for parallel polarization for the in-band scan angle of 30.0 degrees at 18.0 GHz involving the TE_{10}, TE_{20}, TE_{01}, TE_{11}, and TM_{11} waveguide modes.

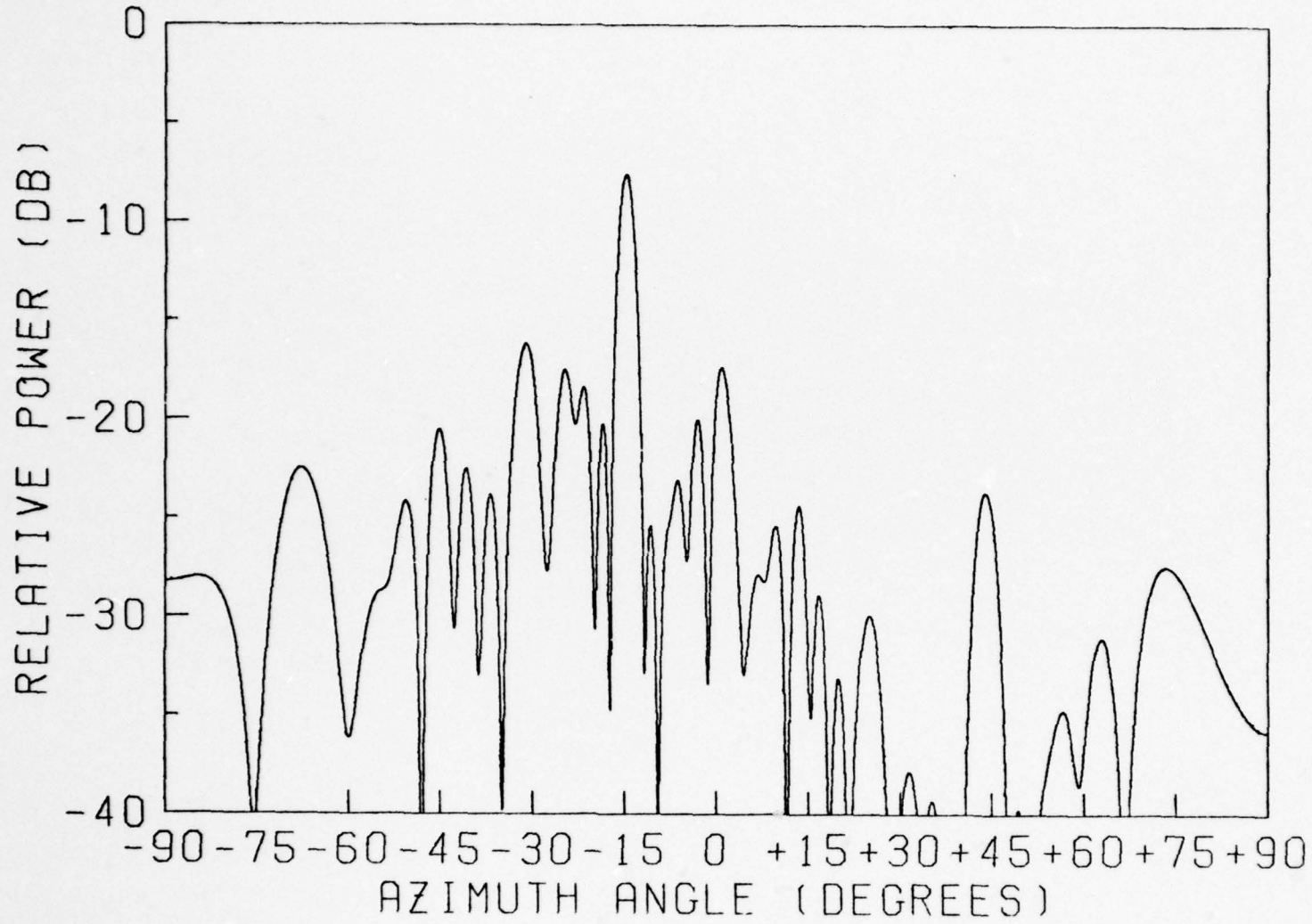

Figure 8. Individual random out-of-band antenna pattern for parallel polarization for the in-band scan angle of 30.0 degrees at 18.0 GHz involving the TE_{10}, TE_{20}, TE_{01}, TE_{11}, and TM_{11} waveguide modes

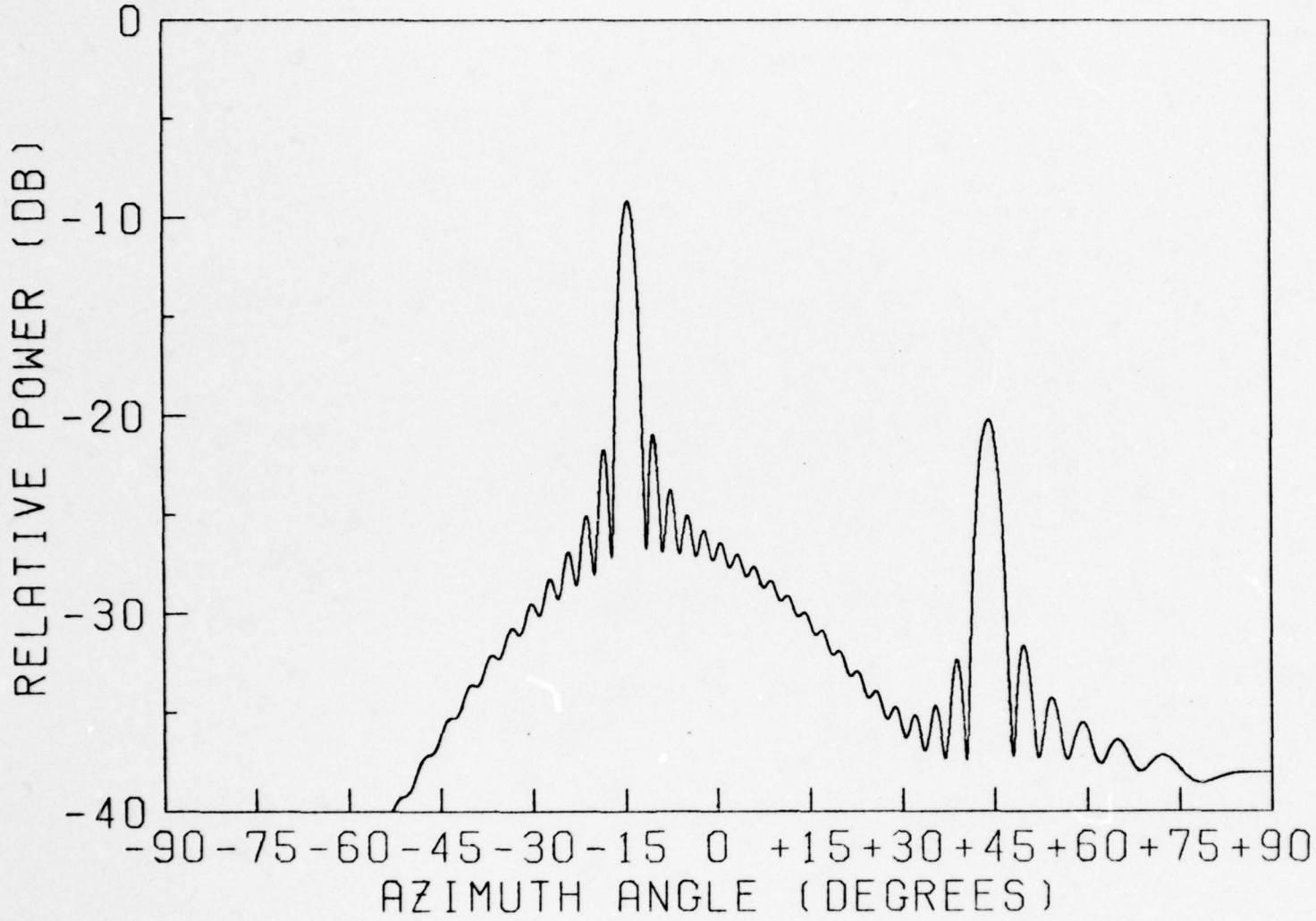

Figure 9. Statistical average out-of-band antenna pattern for cross polarization for the in-band scan angle of 30.0 degrees at 18.0 GHz involving the TE_{10}, TE_{20}, TE_{01}, TE_{11}, and TM_{11} waveguide models.

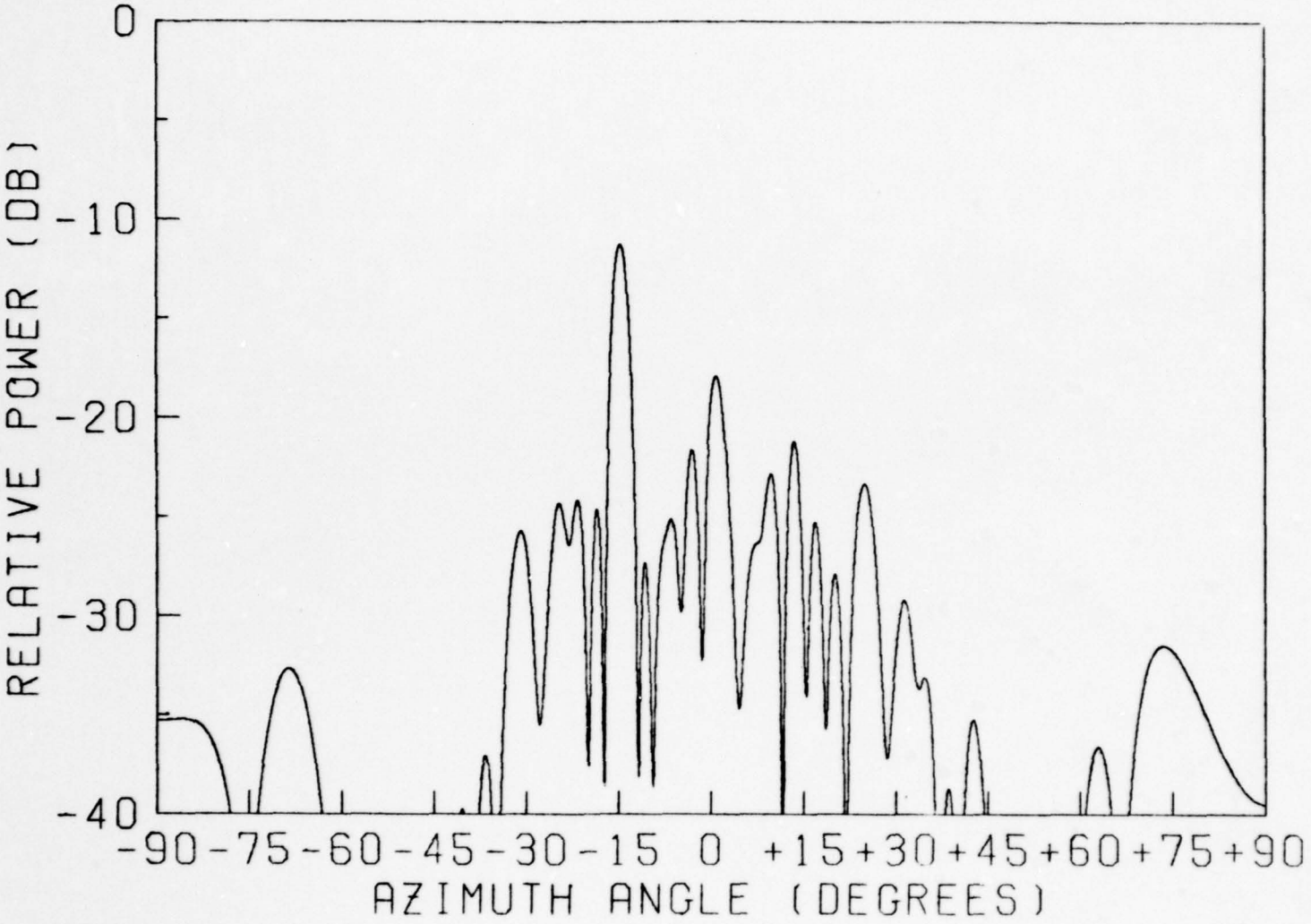

Figure 10. Individual random out-of-band antenna pattern for cross polarization for the in-band scan angle of 30.0 degrees at 18.0 GHz involving the TE_{10}, TE_{20}, TE_{01}, TE_{11}, and TM_{11} waveguide modes.

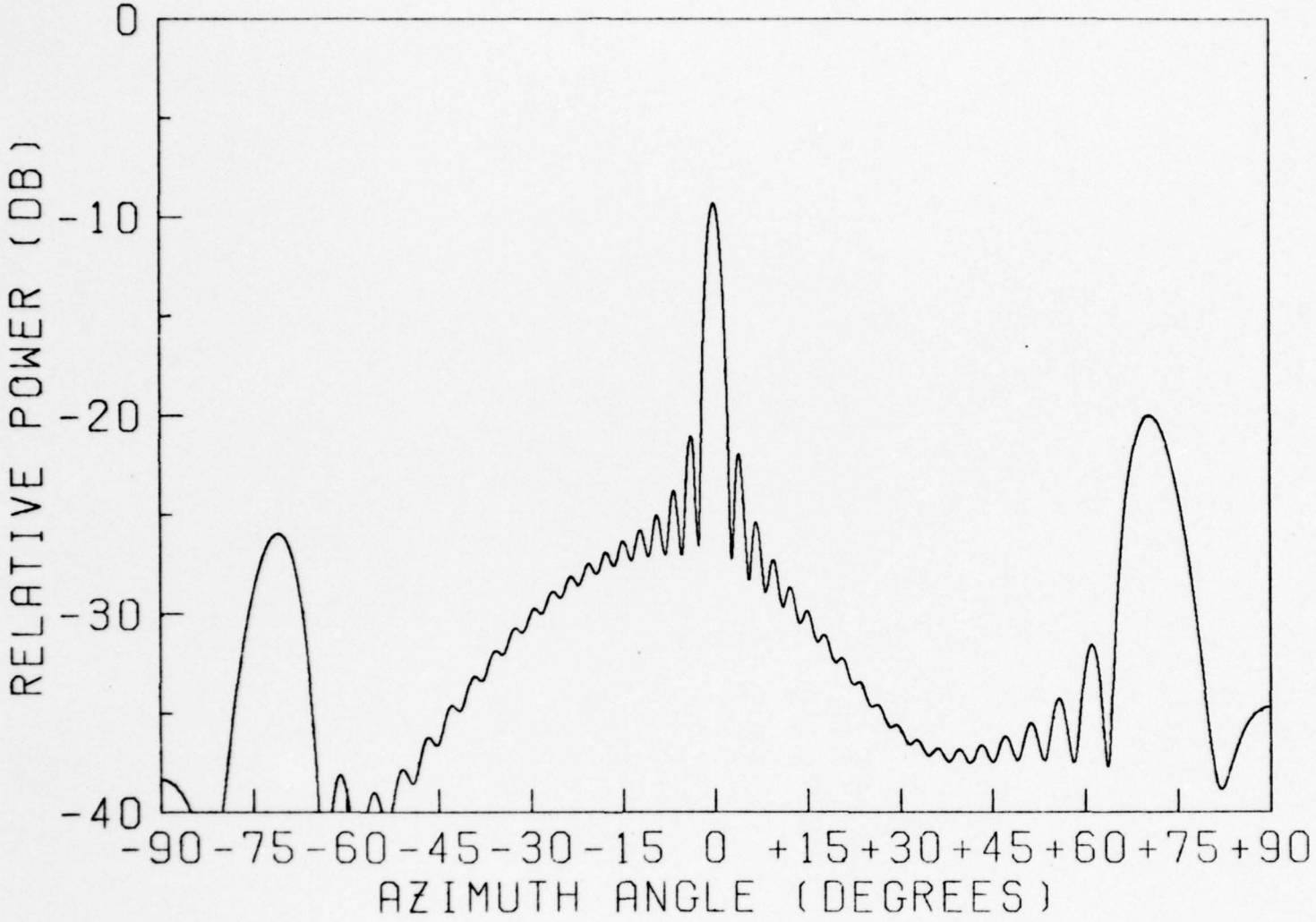

Figure 11. Statistical average out-of-band antenna pattern for parallel polarization for the in-band scan angle of zero degrees at 18.0 GHz involving the TE_{10}, TE_{20}, and TE_{01} waveguide modes.

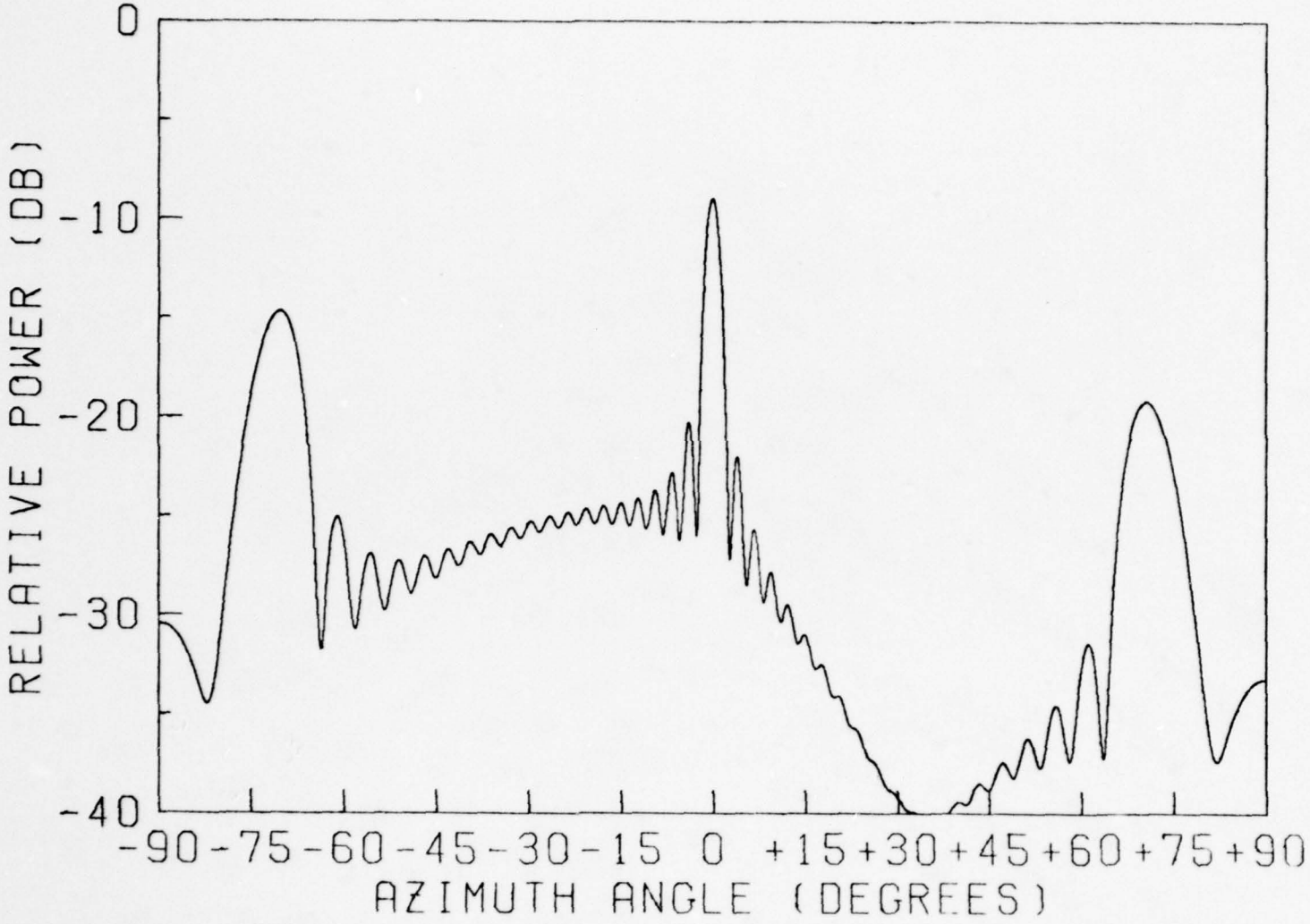

Figure 12. Statistical Average out-of-band antenna pattern for cross polarization for the in-band scan angle of zero degrees at 18.0 GHz involving the TE_{10}, TE_{20}, and TE_{01} waveguide modes

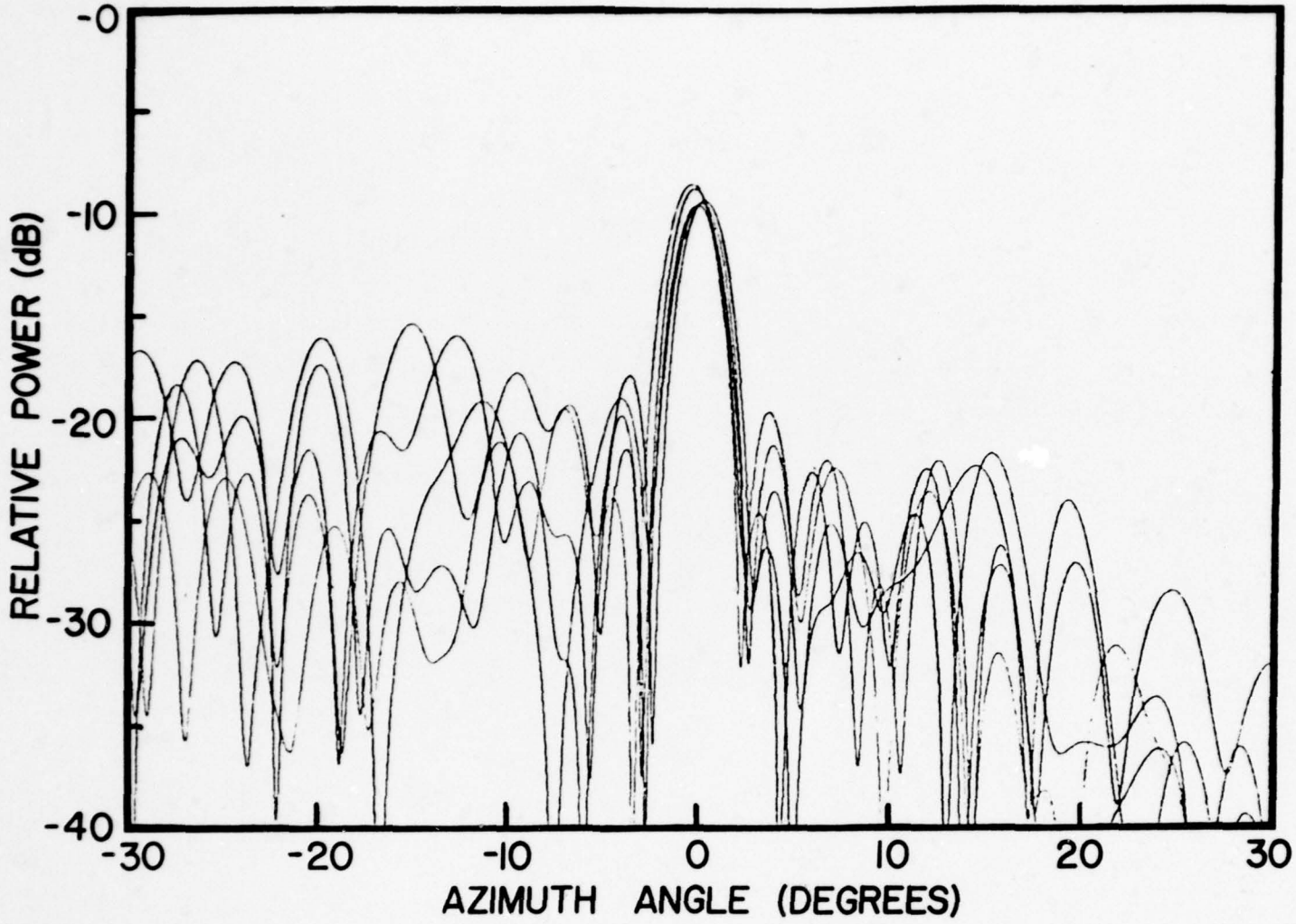

Figure 13. Superposition of the individual random out-of-band antenna pattern for parallel polarization for the out-of-band frequencies of 17.0, 17.5, 18.0, 18.5, and 19.0 GHz.

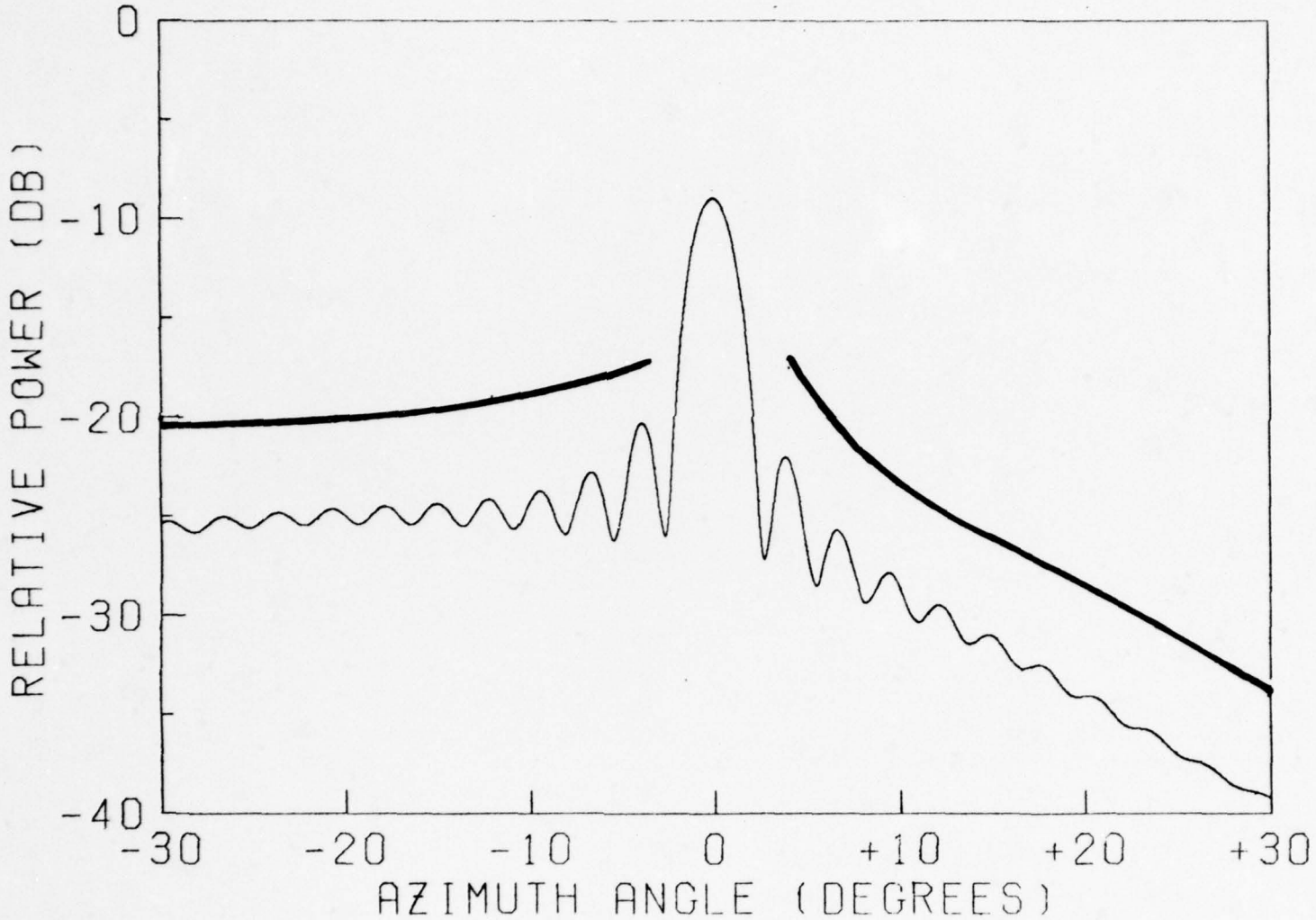

Figure 14. Statistical average pattern and estimated sidelobe standard deviation envelope for parallel polarization for the out-of-band frequency of 18.0 GHz.

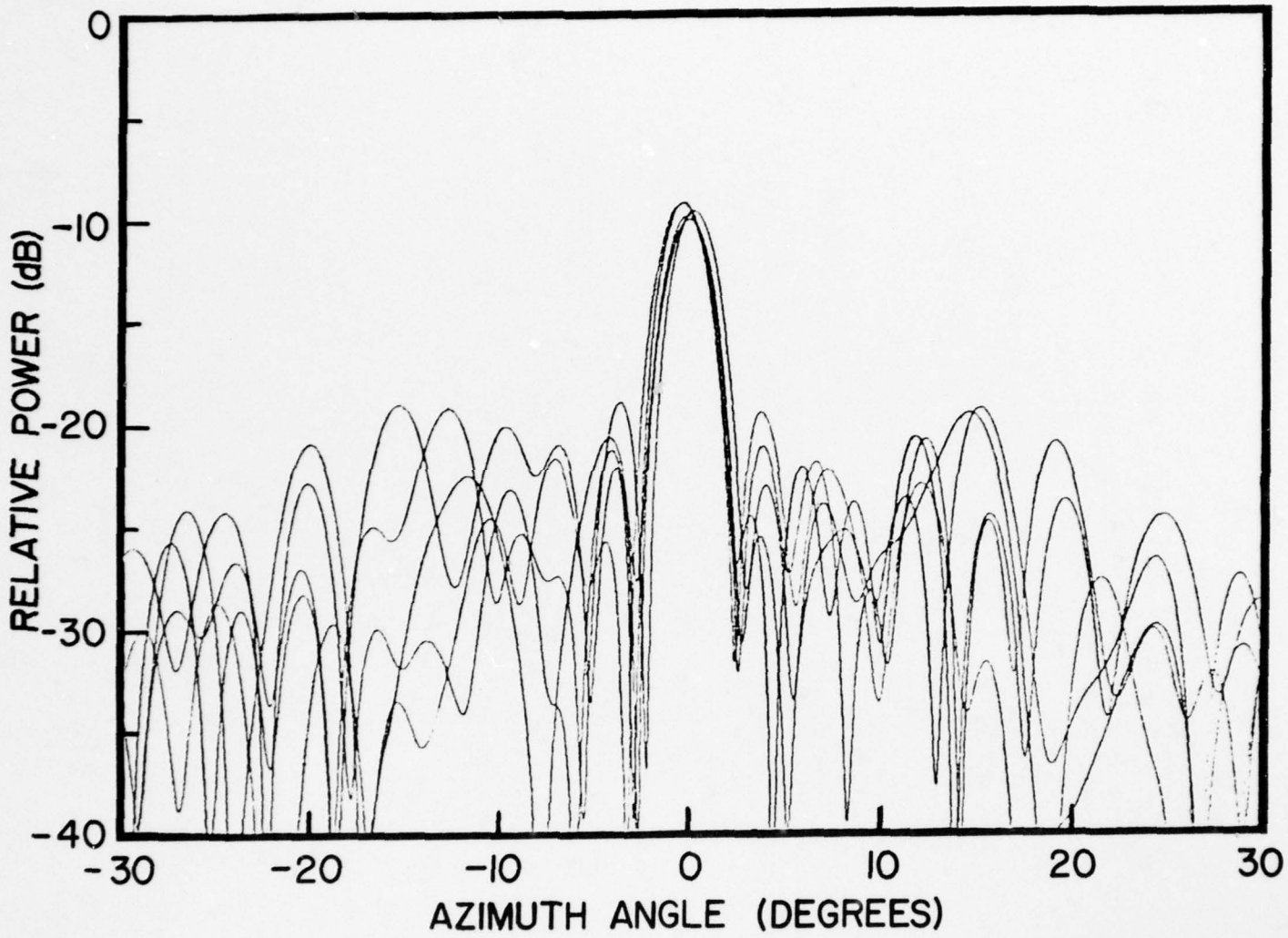

Figure 15. Superposition of the individual random out-of-band antenna pattern for cross polarization for the out-of-band frequencies of 17.0, 17.5, 18.0, 18.5 and 19.0 GHz.

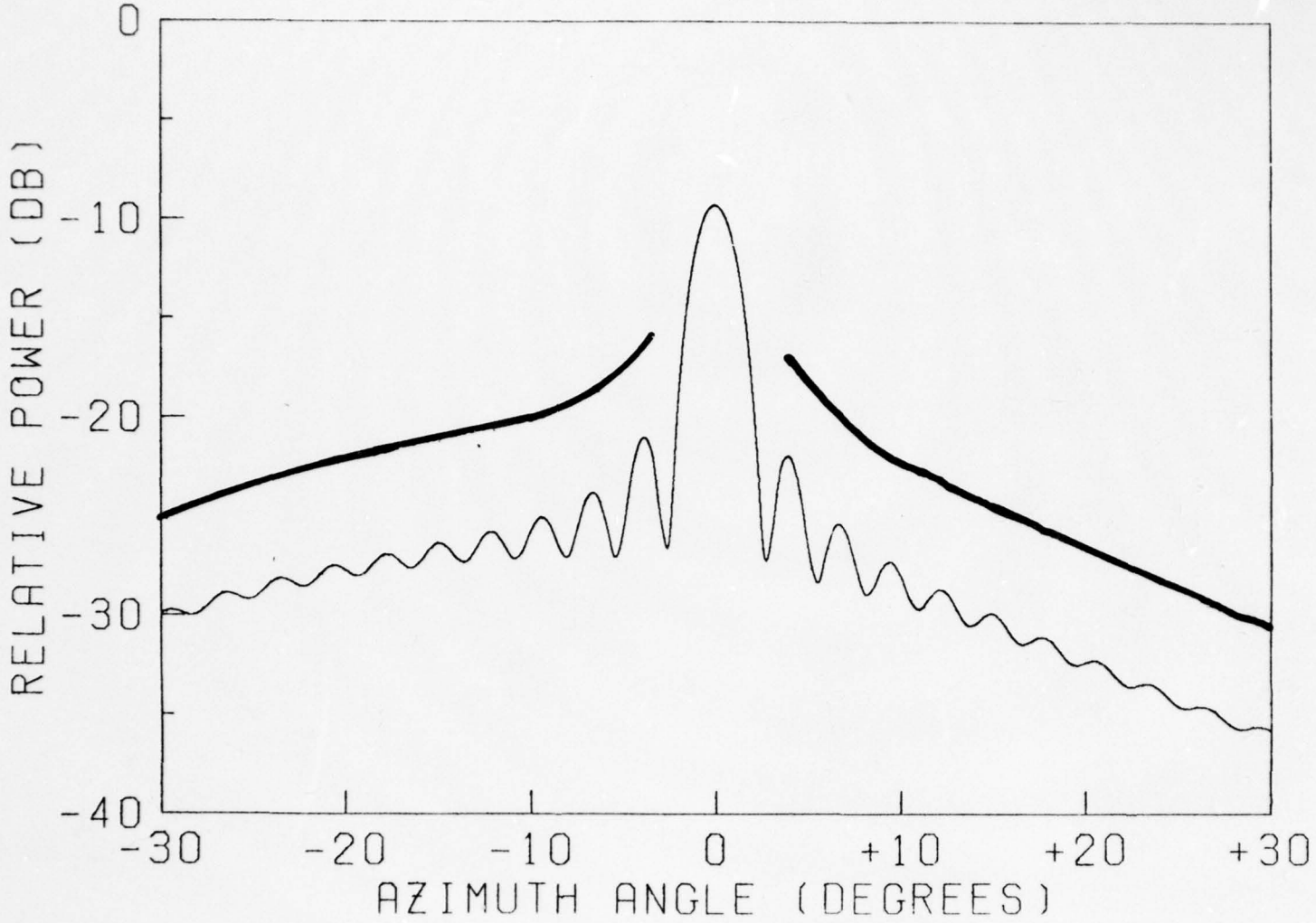

Figure 16. Statistical average pattern and estimated sidelobe standard eviation envelope for cross polarization for the out-of-band frequency of 18.0 GHz.

Inspection of Figures 13 through 16 indicates that the out-of-band statistical average pattern plus statistical standard deviation at the center frequency (18.0 GHz) provides a good engineering description of the out-of-band radiation characteristics over the 2-GHz bandwidth. However, further studies are needed in order to determine the in-band operating conditions and the out-of-band statistical conditions for which this technique is valid. The studies are in progress and the results will be presented and discussed in a future report.

SECTION IV
SUMMARY

A. Analysis

The theory and equations for deriving statistical average out-of-band antenna patterns of wideband and pulsed radiators have been developed. The anlaysis has been conducted for a one-dimensional radiator. However, extension to two-dimensional radiators is straightforward, albeit tedious. The analysis shows that the statistical average pattern for a given frequency is a function of the following near-field statistical parameters:

(1) statistical average value of the electric field at all near-field measurement points,

(2) the standard deviation of the electric field at all measurement points, and

(3) the cross-correlation coefficients of the electric field at all different near-field measurement points.

In a near-field measurement situation, these statistical parameters could be determined by computing appropriate "sample average" values via repeated trials. Alternatively, the statistical parameters can be calculated if the radiating system mode statistics are known from theory or experiment.

A frequency-averaged statistical average pattern for a CW radiating system may be obtained by arithmetically averaging the statistical average patterns over frequency. The frequency average pattern plus standard deviation may be suitable descriptors for a moderate-bandwidth CW radiating system.

The statistical average pattern versus time for a pulsed system depends on all of the above near-field statistical parameters, and the following far-field statistical parameters:

(1) the statistical average value of the far-field electric field at all frequencies in the frequency band,

(2) the standard deviation of the far-field electric field at all frequencies in the frequency band, and

(3) the cross-correlation coefficients of the electric fields at all different frequencies in the frequency band.

Inasmuch as the far-field statistical parameters versus frequency are derivable from the near-field statistical parameters previously cited, the characterization of a pulsed system does not require measurement of any additional near-field statistical parameters.

B. Numerical Simulations

Numerical simulations have been initiated to study the suitability of characterizing a moderate bandwidth CW radiator by the statistical average pattern plus standard deviation for the center frequency in the band. The calculations have been performed for a multi-moding linear array of waveguide elements. Preliminary results are encouraging but further simulations are needed in order to reach valid conclusions. The simulations performed to date have been conducted for the important special case whereby the cross-correlation coefficients of the near-field electric field are all zero.

C. Scheduled Future Efforts

The research efforts will proceed in accordance with the schedule presented on Page 3 in Section I unless redirected by ARO. Accordingly, it is anticipated that Task I will be completed and Task II will be initiated during the reporting period ending June 1979.

Additional numerical simulations will be conducted to define the in-band scan conditions and out-of-band statistical conditions for which the statistical average pattern plus standard deviation at the center frequency is a good descriptor of moderate bandwidth CW radiating systems. Theoretical investigations will also be conducted to derive realistic approximate equations for the cross-correlation functions for both phased array anntennas and reflector antennas. The impact of cross-correlation on measurement complexity can then be assessed.

Theoretical studies will be initiated for Tasks II to derive appropriate statistical equations for predicting coupling between co-sited near-field antennas. It is anticipated that the Plane Wave Spectrum (PWS) technique combined with statistical analysis techniques will be utilized in the derivation.

SECTION V

REFERENCES

1. F.L. Cain, C.E. Ryan, B.J. Cown, and E.E. Weaver, "Electromagnetic Effectiveness Investigations of Near-Field Obstacle Effects, Antenna Coupling, and Phased Arrays," Georgia Institute of Technology, Final Engineering Report, Contract No. N00024-72-C-1274, June 1973.

2. F.L. Cain, B.J. Cown, and E.E. Weaver, "Out-of-Band Frequency Investigations of Near-field Obstacle Effects and Phased Arrays," Georgia Institute of Technology, Final Engineering Report, Contract No. N00024-73-C-1141, February 1974.

3. F.L. Cain, B.J. Cown, E.E. Weaver, and C.E. Ryan, "Far-Field Antenna Performance Concerning In-Band Effects of Near-Field Structures and Out-of-Band Phased Arrays," Georgia Institute of Technology, Final Engineering Report, Contract No. N00024-74-C-1215, January 1975.

4. B.J. Cown, F.L. Cain, and E.F. Duffy, "Statistical Prediction Model for EMC analysis of Out-of-Band Phased Array Antennas," IEEE Transactions on Electromagnetic Compatibility, Vol. EMC-18, No. 4, November 1976.

5. A. Papoulis,, Probability, Random Variables, and Stochastic Processes, McGraw-Hill Book Company 1965.

6. D.T. Paris and F.K. Hurd, Basic Electromagnetic Theory, Chapter 9, McGraw-Hill Book Company, 1969.

7. R.F. Harrington, Time Harmonic Electromagnetic Fields, McGraw-Hill Book Company, 1961.